Optics Communications 95 (1993) 192–198
North-Holland

OPTICS
COMMUNICATIONS

Plane wave expansion of cylindrical functions

G. Cincotti, F. Gori, M. Santarsiero
Dipartimento di Fisica, Università "La Sapienza", P. le A. Moro, 2, 00185 Rome, Italy

F. Frezza, F. Furnò
Dipartimento di Ingegneria Elettronica, Università "La Sapienza", Via Eudossiana, 18, 00184 Rome, Italy

and

G. Schettini
Associazione EURATOM–ENEA sulla Fusione, C.R.E. Frascati, C.P. 65, 00044 Frascati (Rome), Italy

Received 1 July 1992

Cylindrical waves, i.e. the product of a Hankel function of integer order times a sinusoidal angular factor, often occur in diffraction theory. We derive the expansion of a cylindrical wave into plane waves and we give some examples of applications.

1. Introduction

Hankel functions are fundamental building blocks in constructing the solution of many two-dimensional diffraction problems. Let us consider the Helmholtz equation

$$\nabla^2 V + k^2 V = 0\,,$$

where ∇^2 is the two-dimensional Laplace operator and k is the wavenumber of the radiation field. The function V stands for a typical component of the electric or magnetic field. In cylindrical coordinates, the basic solutions of the Helmholtz equation are of the form $H_n(kr)\exp(\mathrm{i}n\alpha)$, where H_n is the Hankel function of integer order n while r and α are a radial and an angular coordinate, respectively. For the sake of brevity, we shall refer to these functions as cylindrical waves of order n (shorthand notation: CW_n). We recall that there are two types of Hankel functions, known as Hankel functions of the first and of the second kind. The corresponding CW_n represents outgoing (first kind) or ingoing (second kind) fields, when a time factor $\exp(-\mathrm{i}\omega t)$ is assumed. Although these functions are so important, their representation in the form of a plane wave expansion is not, to the best of our knowledge, available in the literature, except for the case $n=0$. In this paper, we shall derive such an expansion and we shall give some examples of applications.

Our study was motivated by a research about quasi-optical techniques for launching electromagnetic power into plasmas [1,2]. One of the proposed methods [2] relies on the coupling between the electromagnetic field and the plasma via evanescent waves produced by scattering at a grating. In case the grating is made up by conducting cylinders, the diffracted field can be expressed as a superposition of CW_n. The spatial frequency spectrum of such a field is of interest. Although this can be obtained through numerical Fourier transform

0030-4018/93/$ 06.00

techniques, the knowledge of the spectral representation of CW_n gives substantial benefits. We think that such a knowledge can also be of help for several other diffraction problems.

2. Plane wave expansion of the cylindrical waves

The geometry of our problem is illustrated in fig. 1. Across a certain plane $\eta=\eta_0>0$, we consider a two-dimensional field distribution of the form

$$H_n(\rho)\exp(\mathrm{i}n\alpha), \quad n=0, \pm 1, \pm 2, \ldots, \tag{1}$$

where, for the sake of generality, we use a dimensionless radial coordinate and H_n denotes the Hankel function of integer order n and of the first kind. The latter is generally designated by the symbol $H_n^{(1)}$, in order to distinguish it from the second kind function. Here , we drop the superscript because we do not use functions of both kinds at the same time. We want to express the above distribution as a superposition of plane waves.

Out starting point is the following Sommerfeld integral representation [3] for the Hankel functions of the first kind

$$H_n(\rho)=\frac{(-\mathrm{i})^n}{\pi}\int_C \exp(\mathrm{i}\rho\cos w+\mathrm{i}nw)\,\mathrm{d}w, \tag{2}$$

where the integral is to be evaluated in the plane of the complex variable

$$w=u+\mathrm{i}v, \tag{3}$$

and the integration path C can be shaped as in fig. 2. The precise form of C can be chosen with some arbitrariness. The basic requirements are as follows: (i) C passes through the origin; (ii) the upper path ($v>0$) belongs to the vertical strip $-\pi<u\leqslant 0$; (iii) the lower path ($v<0$) belongs to the vertical strip $0\leqslant u<\pi$. For a typical point P on the chosen plane (see fig. 1), we have $0<\alpha<\pi$. We then exploit the allowed freedom in the choice of the integration path letting it to assume the form C' shown in fig. 2. The integral appearing in eq. (2) can then be divided into three contributions as follows

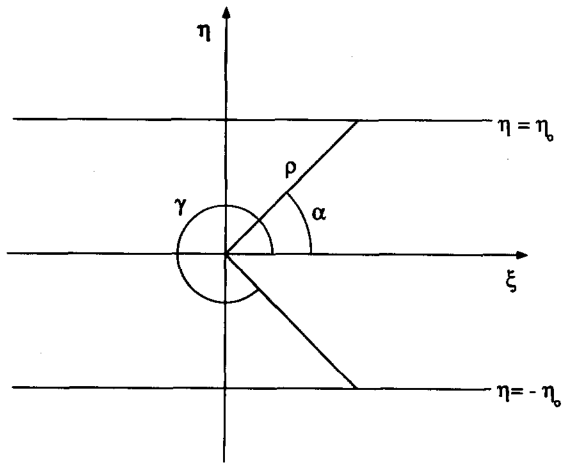

Fig. 1. Coordinate system used in this paper.

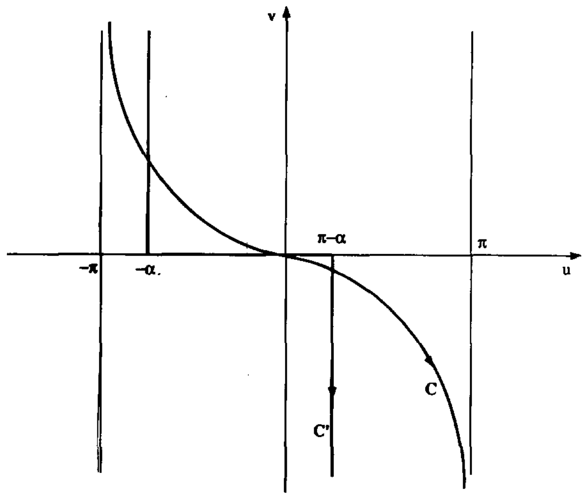

Fig. 2. Two possible integration paths for the evaluation of the function $H_n(\rho)$ in eq. (2).

$$H_n(\rho)=\frac{(-i)^n}{\pi}\left(i\int_{\infty}^{0}\exp[i\rho\cos(-\alpha+iv)+in(-\alpha+iv)]\,dv+\int_{-\alpha}^{\pi-\alpha}\exp(i\rho\cos u+inu)\,du\right.$$

$$\left.+i\int_{0}^{-\infty}\exp[i\rho\cos(\pi-\alpha+iv)+in(\pi-\alpha+iv)]\,dv\right). \tag{4}$$

By simple change of variables eq. (4) can be transformed into the following one

$$H_n(\rho)\exp(in\alpha)=\frac{(-i)^n}{\pi}\left(-i\int_{0}^{\infty}\exp[i\rho\cos(\alpha-iv)-nv]\,dv+\int_{0}^{\pi}\exp[i\rho\cos(u-\alpha)+inu]\,du\right.$$

$$\left.-i(-1)^n\int_{-\infty}^{0}\exp[-i\rho\cos(\alpha-iv)-nv]\,dv\right), \tag{5}$$

where the CW_n is now evidentiated on the left hand side. On expanding the cosine functions, eq. (5) becomes

$$H_n(\rho)\exp(in\alpha)=\frac{(-i)^n}{\pi}\left(-i\int_{0}^{\infty}\exp(i\rho\cos\alpha\cosh v-\rho\sin\alpha\sinh v-nv)\,dv\right.$$

$$+\int_{0}^{\pi}\exp(i\rho\cos\alpha\cos u+i\rho\sin\alpha\sin u+inu)\,du$$

$$\left.-i(-1)^n\int_{-\infty}^{0}\exp(-i\rho\cos\alpha\cosh v+\rho\sin\alpha\sinh v-nv)\,dv\right). \tag{6}$$

We now use the cartesian coordinates ξ and η shown in fig. 1. Equation (6) can then be expressed in the form

$$H_n(\rho)\exp(in\alpha)=\frac{(-i)^n}{\pi}\left(-i\int_{0}^{\infty}\exp(i\xi\cosh v-\eta_0\sinh v-nv)\,dv\right.$$

$$\left.+\int_{0}^{\pi}\exp(i\xi\cos u+i\eta_0\sin u+inu)\,du-i(-1)^n\int_{0}^{\infty}\exp(i\xi\cosh v-\eta_0\sinh v+nv)\,dv\right), \tag{7}$$

where the change $v\to -v$ has been made in the last integral. The hypothesis $\eta_0>0$ ensures convergence of the first and third integrals because $-\eta_0\sinh v$ is the dominant term in the exponent. The functions $\cosh(v)$ and $\cos(u)$ can be inverted in $[0,\infty)$ and $[0,\pi]$, respectively. Accordingly, we let

$$v=\ln(\sqrt{\beta^2-1}+\beta) \tag{8}$$

in the first and third integrals and

$$v=\cos^{-1}\beta \tag{9}$$

in the second one. The following relation is then obtained from eq. (7)

$$H_n(\rho)\exp(in\alpha)=\frac{(-i)^n}{\pi}\left(\int_1^\infty \frac{\exp(i\beta\xi-\eta_0\sqrt{\beta^2-1})}{(\sqrt{\beta^2-1}+\beta)^n}\frac{d\beta}{i\sqrt{\beta^2-1}}\right.$$

$$+\int_{-1}^{1}\exp(i\beta\xi+i\eta_0\sqrt{1-\beta^2}+in\cos^{-1}\beta)\frac{d\beta}{\sqrt{1-\beta^2}}$$

$$\left.+(-1)^n\int_{-\infty}^{-1}\exp(i\beta\xi-\eta_0\sqrt{\beta^2-1})\,(\sqrt{\beta^2-1}-\beta)^n\frac{d\beta}{i\sqrt{\beta^2-1}}\right). \tag{10}$$

Equation (10) contains the required result. In fact, it can be given the form

$$H_n(\rho)\exp(in\alpha)=\int_{-\infty}^{\infty}F_n(\beta,\eta_0)\exp(i\beta\xi)\,d\beta,\quad \xi=\rho\cos\alpha,\quad \eta=\eta_0=\rho\sin\alpha>0\,, \tag{11}$$

where

$$\begin{aligned} F_n(\beta,\eta_0)&=\frac{(i)^{n-1}}{\pi}\frac{\exp(-\eta_0\sqrt{\beta^2-1})\,(\sqrt{\beta^2-1}-\beta)^n}{\sqrt{\beta^2-1}}, && -\infty<\beta<-1\,,\\ &=\frac{(-i)^n}{\pi}\frac{\exp(i\eta_0\sqrt{1-\beta^2}+in\cos^{-1}\beta)}{\sqrt{1-\beta^2}}, && -1<\beta<1,\\ &=\frac{(-i)^{n+1}}{\pi}\frac{\exp(-\eta_0\sqrt{\beta^2-1})}{(\sqrt{\beta^2-1}+\beta)^n\sqrt{\beta^2-1}}, && 1<\beta<\infty\,. \end{aligned} \tag{12}$$

The CW_n is now expressed as a Fourier integral with respect to the variable ξ. As well known [4], this is equivalent to representing the field produced by the CW_n across the plane $\eta=\eta_0>0$ as a superposition of both homogeneous and non-homogeneous (or evanescent) waves. More precisely, homogeneous waves correspond to the interval $|\beta|<1$.

Up to now, we assumed $\eta_0>0$. However, it is not difficult to extend our result to the case $\eta_0<0$. With reference to fig. 1, we note that the field produced at (ξ,η_0) by the CW_n is

$$H_n(\rho)\exp(in\gamma)\,. \tag{13}$$

It is seen that the same field can be written as

$$H_n(\rho)\exp(-in\alpha)=(-1)^n H_{-n}(\rho)\exp(-in\alpha)\,. \tag{14}$$

This means that the field at (ξ,η_0) is $(-1)^n$ times the field that would be produced at $(\xi,|\eta_0|)$ by the cylindrical wave of order $-n$. The following rule then holds

$$F_n(\beta,\eta_0)=(-1)^n F_{-n}(\beta,|\eta_0|),\quad \eta_0<0\,. \tag{15}$$

We further note that for $n=0$ eq. (10) reduces to a known formula [5].

In fig. 3, we give the curves of the modulus of $F_n(\beta,\eta_0)$ for $n=1$ and $\eta_0=0.1$ (full line), $\eta_0=0.25$ (dashed line), and $\eta_0=0.5$ (dotted line). In fig. 4, curves are plotted for a fixed value of η_0 ($\eta_0=0.5$) and different values of n ($n=0$, full line; $n=1$, dashed line; $n=2$, dotted line). It can be seen that the relative weight of the evanescent waves increases when η_0 becomes smaller and when n becomes greater.

As a final remark, we add that the case of ingoing cylindrical waves can similarly dealt with because the Hankel functions of the second kind are simply the complex conjugate of those of the first kind.

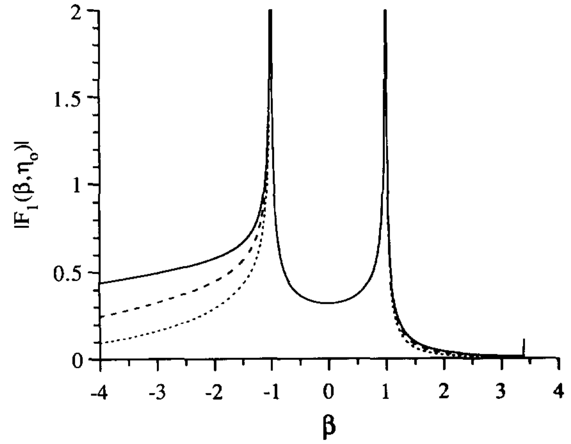

Fig. 3. Modulus of $F_1(\beta, \eta_0)$ for $\eta_0=0.1$ (full line), $\eta_0=0.25$ (dashed line) and $\eta_0=0.5$ (dotted line).

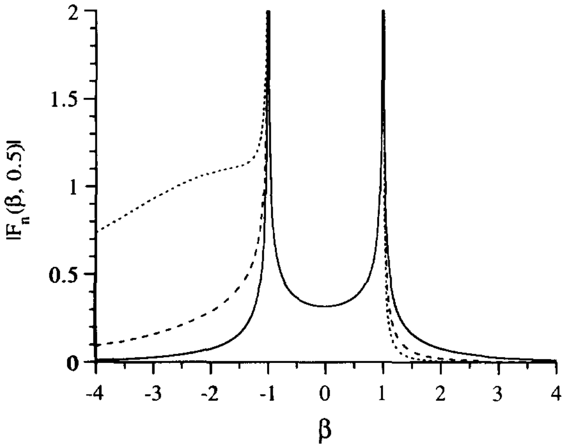

Fig. 4. Modulus of $F_n(\beta, \eta_0=0.5)$ for $n=0$ (full line), $n=1$ (dashed line) and $n=2$ (dotted line).

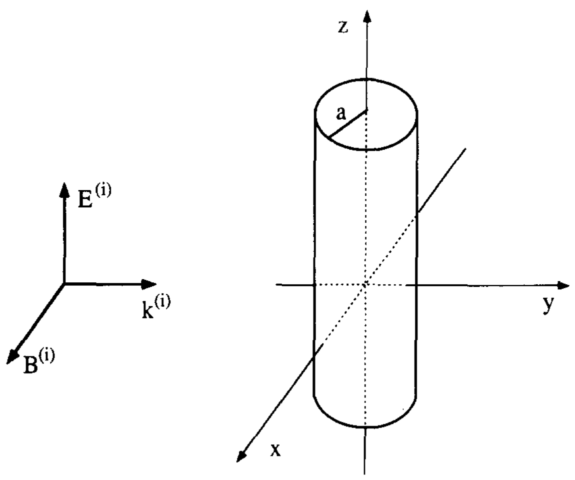

Fig. 5. Description of the geometry for the scattering of a plane wave from a circular cylinder.

3. Diffraction of a plane wave by conducting cylinders

The basic diffraction in which CW_n are involved refers to a single circular cylinder illuminated by a plane wave. Several other two-dimensional problems of diffraction rely on the results obtained in the previous case. We quote, for example, diffraction from a conducting wire grating and diffraction from a set of conducting cylinders with various radii. Furthermore, a conducting surface that can be approximated by a set of closely spaced wires [6] and this gives rise to a widely used technique for finding approximate solutions of a lot of two-dimensional diffraction problems. Some basic properties of the field diffracted by a single cylinder are carried over the solution of the more complicated problems. Accordingly, it may be helpful to use the results of the previous section in order to outline some features of the spectrum of plane waves that is produced by diffraction at a single cylinder.

Suppose that a linearly polarized, monochromatic plane wave is orthogonally incident on a perfectly conducting circular cylinder of radius a (fig. 5). Let us assume that the electric field vector $\boldsymbol{E}^{(i)}$ of the wave is parallel to the cylinder axis (E polarization). The problem is of scalar nature. For the sake of simplicity, we assume that the y-axis is parallel to the propagation direction of the incident wave. The diffracted field, say $E^{(d)}$, can be expressed as a series of CW_n as follows [7]

$$E^{(d)}(r, \alpha) = \sum_{n=-\infty}^{\infty} c_n H_n(kr) \exp(in\alpha) , \tag{16}$$

where r and α are polar coordinates in the (x, y)-plane. The coefficients c_n can be easily found and turn out to be

$$c_n = -J_n(ka)/H_n(ka) , \tag{17}$$

where J_n is the Bessel function of integer order n and of the first kind. For increasing $|n|$ the moduli of the c_n tend to get smaller and smaller, possibly in a non-monotonic way. As a rule of thumb, for $ka > 1$ the c_n become negligible when $|n| > 3ka$. For $ka < 1$, the c_n become very small when $|n|$ exceeds a few units (say 3 or 4). The angular spectrum of the field given by eq. (16) can be evaluated by means of eqs. (11) and (12), by taking into account that ρ, ξ and η are replaced by kr, kx and ky respectively.

In fig. 6 we show the modulus of the angular spectrum $A_E(\beta)$ of the field $E^{(d)}$ in arbitrary units, for three different values of the cylinder radius: $ka=0.15$ (full line), $ka=3.14$ (dashed line) and $ka=12.56$ (dotted line), evaluated on a plane placed at a distance $ky=1.5ka$ from the cylinder axis. It is seen that increasing ka the radiation pattern becomes more and more anisotropic. At the same time the weight of the evanescent components diminishes.

The complementary case of H polarization (H vector parallel to the x-axis) can be treated in a similar manner. The function E is replaced by H in eq. (16). The boundary conditions then lead to an expression analogue to eq. (17), where instead of the J_n and H_n functions the respective derivatives appear.

The previously discussed problem can be generalized to the case of scattering by an arbitrary arrangement of circular cylinders, having parallel, non-coplanar axes and possibly different radii. The field radiated by the jth element of the arrangement, say $E_j^{(d)}$, can again be expressed as a superposition of CW_n of the form (16). The values of the corresponding expansion coefficients, say c_{jn}, are then obtained through the solution of a set

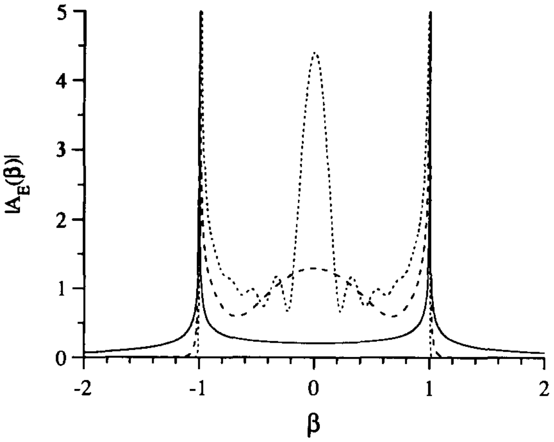

Fig. 6. Modulus of the angular spectrum of the field diffracted by a single cylinder for three different radii: $ka=0.15$ (full line), $ka=3.14$ (dashed line) and $ka=12.56$ (dotted line) evaluated at a distance $ky=1.5ka$.

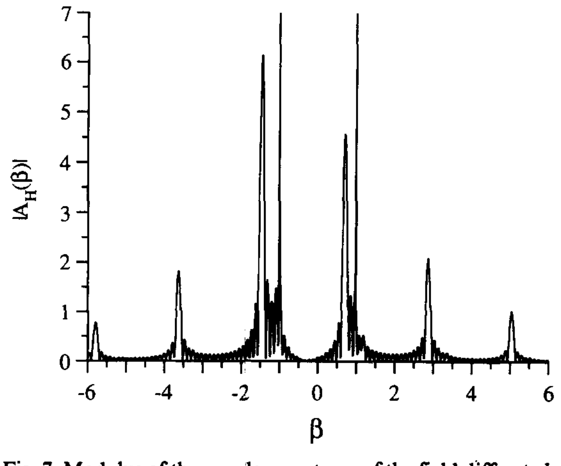

Fig. 7. Modulus of the angular spectrum of the field diffracted at 5 GHz by an array of 20 cylinders with 3 mm radius ($ka=0.3$), spaced by 28 mm ($kd=2.9$) and evaluated on a plane at 3.5 mm ($kh=0.35$) from their axes. The grating is illuminated by a plane wave at a 45° incidence angle.

of linear equations, which arises from the application of suitable boundary conditions [8]. In this way, by means of the plane wave expansion of the CW_n (eq. (11)), the angular spectrum of the field diffracted by the whole structure is obtained. Obviously, this is of relevant interest in the investigation of structures endowed with particular scattering properties.

As an example, we show the results concerning a rather simple, but very significant arrangement: N circular cylinders with coplanar and equidistant axes and equal radii. Such a structure is often referred to as a finite array of cylinders. As we said in the introduction, the use of a grating of this type has been suggested [2] as a mean for coupling a microwave beam to the so called Lower Hybrid wave of a plasma through the evanescent waves produces by scattering at the grating. Taking into account the experimental requirements for the Lower Hybrid heating of the plasma [1], we analysed a structure that produces, in vacuo, an angular spectrum with one prevalent diffraction order in the evanescent wave region ($|\beta| > 1$). To this aim the choice of H polarization leads to better results, because in this case the coupling with the slow wave of the plasma is more efficient; moreover, the power losses on the conducting cylinders are lower and the current distributions induced on the conducting surfaces produce spatially more rapidly varying fields, corresponding to angular spectra with high frequency components of larger amplitude. A typical result is shown in fig. 7. Here, we plotted the modulus of the angular spectrum $A_H(\beta)$ of the field diffracted by a finite array of 20 cylinders with radius $a=3$ mm whose axes are spaced by $d=28$ mm. A plane wave with 5 GHz temporal frequency illuminates the grating at a 45 degree incidence angle. After solving numerically for the c_{jn} coefficients defined above, we computed the angular spectrum at a distance $h=3.5$ mm from the grating by means of eq. (12). It is seen that the largest component of the spectrum lies in the evanescent wave region as required by the coupling problem.

References

[1] R.A. Cairns, Radiofrequency heating of plasmas (Adam Hilger, Bristol, 1991) Ch. 4.
[2] M.I. Petelin and E.V. Suvorov, Sov. Techn. Phys. Lett. 15 (1989) 882.
[3] A. Sommerfeld, Partial differential equations in physics (Academic Press, New York, 1964) Ch. 4.
[4] M. Born and E. Wolf, Principles of optics (Pergamon Press, Oxford, 1980) Ch. 11.
[5] I.S. Gradshteyn and I.M. Ryzhik, Table of Integrals, Series, and Products (Academic Press, New York, 1980) Ch. 8.
[6] J.H. Richmond, IEEE Trans. Microwave Theory Tech. 13 (1965) 408.
[7] C.A. Balanis, Advanced engineering electromagnetics (Wiley, New York, 1989) Ch. 11.
[8] H.A. Ragheb and M. Hamid, Int. J. Electron. 59 (1985) 407.